

Role of Susceptibility Weighted Imaging in Evaluation of Gynecological Diseases

Thesis

Submitted for Partial Fullfillment of Master Degree in Radiodiagnosis

Presented by Beshoy Samuel Fawzy

(M.B.B.C.H)
Faculty of Medicine
Ain Shams University

Supervised by

Prof.Dr. Sherine George Moftah

Professor of Radiology Faculty of Medicine Ain Shams University

Dr. Wafaa Rafaat Abd El Hamid

Lecturer of Radiology Faculty of Medicine Ain Shams University

Faculty of Medicine
Ain Shams University
2018

Acknowledgment

First and foremost, praise is to **God**, to whom I relate any success in achieving any work in my life.

I wish to express my deepest thanks, gratitude and appreciation to **Prof. Dr. Sherein George Moftah** for her sincere encouragement, constant advice and valuable guidance throughout the performance of this work.

I owe special thanks to **Dr. Wafaa Rafaat Abd El Hamid** for her kind care and help throughout this work.

I would like to thank my professors, my family, and my colleagues, for their support and moral encouragement.

Beshoy Samuel Fawzy

List of Contents

Title	Page No.
List of Tables	4
List of Figures	5
List of Abbreviations	9
Introduction	1
Aim of the Study	14
Review of Literature	
 Anatomy of Female Reproductive System 	15
 Pathology of Gynecologic Hemorrhagic Diseas 	es26
 Magnetic Resonance Imaging Technique in F Pelvis Examination 	
 Imaging of Gynecologic Hemorrhagic Diseases 	s57
Patients and Methods	84
Results	87
Illustrated Cases	98
Discussion	108
Summary and Conclusion	114
References	116
Arabic Summary	

List of Tables

Table No.	Title Pag	e No.
Table (1):	Most Common Sites for Endometrioti	
	Implants and Adhesions	
Table (2):	The main characteristics differentiating	_
	adenomyosis from leiomyoma by MRI	76
Table (3):	Relation between susceptibility weighte	
	imaging (SWI) and uterine lesions:	88
Table (4):	Relation between susceptibility weighte	d
	imaging (SWI) and ovarian lesions	89
Table (5):	Relation between susceptibility weighte	d
	imaging (SWI) and pelvic lesions	90
Table (6):	Relation between susceptibility weighte	
	imaging (SWI) and the hemorrhagic lesions	91
Table (7):	Relation between susceptibility weighte	
	imaging (SWI) and T1 signal intensity	
Table (8):	Relation between susceptibility weighte	
	imaging (SWI) and T2 signal intensity	
Table (9):	Relation between susceptibility weighte	
	imaging (SWI) and diffusion weighte	
	imaging.	
Table (10):	Diagnostic Performance of SWI in reference	
_ 3,020 (20)	to conventional MRI.	

List of Figures

Fig. No.	Title Po	ige No.
Fig. (1):	Female reproductive organs	15
Fig. (2):	Diagram of the normal uterine muscles	17
Fig. (3):	Luteal phase and Menstrual pha	ıse
	endometrium	18
Fig. (4):	Diagram showing the uterus and associat	ed
	ligaments	20
Fig. (5):	Blood supply of the uterus. Posterior view	22
Fig. (6):	Showing normal anatomy of the fema	ale
	reproductive system	23
Fig. (7):	Showing blood supply of ovary	25
Fig. (8):	Large hemorrhagic cyst macroscopic pictu	re27
Fig. (9):	Endometrial implants outside uterine cav	-
	(Endometriosis)	
Fig. (10):	Ovarian endometriosis with chocolate cy	
	appearance	
Fig. (11):	Drawing illustrates ectopic endometry	
	glands	
Fig. (12):	Adenomyosis	
Fig. (13):	The FIGO leiomyoma subclassificati	
	system	
Fig. (14):	Uterine fibroids	
Fig. (15):	MRI pelvis body coil	
Fig. (16):	Subtraction of pre- and post-contrast T	
T • (4 F)	weighted images	
Fig. (17):	DWI in a 26-year-old patient with suspect	
T! (10)	deep infiltrating enometriosis	
Fig. (18):	Sequence of events in 3D long TE gradie	
	echo MR imaging with flow compensation	
E! - (10)	all three directions	
Fig. (19):	Left- and right-handed coordinate systems	
Fig. (20):	Steps of image reconstruction susceptibility weighted imaging	
	susceptibility weighted illiaging	5 <i>Z</i>

List of Figures Cont...

Fig. No.	Title	Page No.
Fig. (21):	27 year-old patient with endometriotic in the left ovary	-
Fig. (22):	47-year-old woman with right-sided ov endometrioma	arian
Fig. (23):	46-year-old woman with right-sided overdometrioma	
Fig. (24):	39-year-old woman with left-sided overdometrioma	
Fig. (25):	Ruptured hemorrhagic cyst	
Fig. (26):	Bilateral endometriomas in a 21-ye woman	ear-oid 60
Fig. (27):	Bilateral endometriomas in a 46-year woman	61
Fig. (28):	33-year-old woman with endometrion left ovary	
Fig. (29):	26-year-old woman with ovarian and endometriosis	
Fig. (30):	Endometriotic cysts (chocolate cysts) 30-year-old woman	
Fig. (31):	38-year-old woman with left-sided ov dermoid cyst, endometrioma, and sided ovarian corpus luteum	right-
Fig. (32):	Diffuse adenomyosis with hemorrh submucosal microcysts	hagic,
Fig. (33):	A 28-year-old woman with adenom who presents with pelvic pain menorrhagia	and
Fig. (34):	Direct and indirect features of adenomy	osis71
Fig. (35): Fig. (36):	Adenomyotic cyst Adenomyosis with leiomyomas	
Fig. (37):	Typical leiomyoma	
Fig. (38):	A 45-year-old woman with large ut leiomyoma	terine

List of Figures Cont...

Fig. No.	Title Page	No.
Fig. (39):	A 33-year-old woman with pedunculated leiomyoma	80
Fig. (40):	A 30-year-old pregnant woman with	
	transient uterine contraction and pelvic	
T' - (41)	pain	81
Fig. (41):	A 28-year-old woman with adenomyoma	
	who presents with pelvic pain and menorrhagia	82
Fig. (42):	A 45-year-old woman with endometrial	02
g· (-=/·	polyp and irregular menstrual bleeding	83
Fig. (43):	Bar chart between susceptibility weighted	
	imaging (SWI) and T1 signal intensity	92
Fig. (44):	Bar chart between susceptibility weighted	
	imaging (SWI) and T2 signal intensity	94
Fig. (45):	Bar chart between susceptibility weighted	
	imaging (SWI) and diffusion weighted imaging.	06
Fig. (46):	Axial T1W and axial T2W	
Fig. (47):	Axial SWI	
Fig. (48):	Axial T2 WIs and Axial T1 WIs	
Fig. (49):	Axial SWI	99
Fig. (50):	Axial DWI and ADC map images	100
Fig. (51):	Axial A,B and sagittal C images	
Fig. (52):	Axial SWI	
Fig. (53):	Axial T1W and Axial T2W	
Fig. (54): Fig. (55):	Axial SWI Axial DWI and ADC map images	
Fig. (56):	Coronal and axial T2WIs and axial T1WI	
Fig. (57):	Axial SWI	
Fig. (58):	Axial T1WI and Axial, coronal T2WIs	
Fig. (59):	Axial SWI	
Fig. (60):	Axial DWI and ADC map images	106

List of Figures Cont...

Fig. No.	Title	Page No.
Fig. (61):	Axial T1 and Axial T2WIs	107
•	Axial SWI	

List of Abbreviations

Abb. Full term

ADC	Apparent Diffusion Coeffici	ient	
DWI	Diffusion Weighted Images		
<i>EPI</i>	Echo-Planar Imaging		
HASTE	Half-Fourier Acquisition Spin-Echo	$Single ext{-}Shot$	Turbo
MRI	Magnetic Resonance Imagi	ng	
MS	Multi-Shot		
<i>RF</i>	Radio-Frequency		
SNR	Signal to Noise Ratio		
SS	Single Shot		
SWI	Susceptibility Weighted Im	aging	
<i>TM</i>	Trademark		
TSE	Turbo Spin Echo		



INTRODUCTION

agnetic resonance imaging (MRI) is a rapidly evolving Limaging modality, which over the last decade with the development of increasingly faster sequences and methods of image processing was used in the evaluation of gynecological diseases. Newer techniques introduced in the pelvic MRI such susceptibility-weighted imaging (SWI), spectroscopy, diffusion-weighted imaging, and functional imaging have future applications (Reston, et al., 2006).

Susceptibility-weighted imaging (SWI) is an MRI sequence which is particularly sensitive to compounds which distort the local magnetic field and as such make it useful in detecting blood products, calcium etc. It has been used in imaging of central nervous system and recently in body and pelvis imaging too (Wu et al., 2009).

SWI uses a fully flow compensated, long echo, gradient recalled echo (GRE) pulse sequence to acquire images. This method exploits the susceptibility differences between tissues and uses the phase image to detect these differences. The magnitude and phase data are combined to produce an enhanced contrast magnitude image which is exquisitely sensitive to venous blood, hemorrhage and iron storage (*Deistung et al.*, 2008).



The magnetic susceptibility effects generated by local inhomogeneity of the magnetic field are visualized as signal voids. SWI not only detects subacute blood products like methemoglobin, but also acute and chronic blood products such as deoxyhemoglobin and hemosiderin (Krishnan et al., 2015).

SWI is sensitive for the presence of hemorrhage within various gynecologic pathologies and helpful for the differential diagnosis such as: Hemorrhagic ovarian cysts, Endometriosis, pregnancy, Hemorrhagic Uterine Ectopic pathologies (Adenomyosis with hemorrhagic foci, Leiomyomas with red degeneration, with hemorrhagic necrosis, and Placental polyp with hemorrhagic foci) (Krishnan et al., 2015).

Hemorrhagic ovarian cysts show high signal intensity on T1WI and high signal intensity on SWI (water-like pattern). No flow voids along the cyst wall is observed on SWI. Acute intracystic hemorrhage may show low intensity both on T1WI (no methemoglobin) and SWI (due to deoxyhemoglobin). Because SWI is sensitive to a small amount of hemorrhagic contents, SWI may be able to differentiate mucinous cysts from hemorrhagic cysts both exhibiting high signal intensity on T1WI (*Rajkotia et al.*, 2006).

Endometriosisis a common chronic disease affecting young women, repeated cyclic bleeding and rupture of endometriomas can cause severe pelvic adhesions and infertility, so early diagnosis is important for the adequate



treatment. Definite MR criteria are as follows: 1) Multiple T1high cysts (multiplicity) and/or 2) T1-high /T2-low cyst (shading). However, some endometriomas do not meet the criteria, and it may be difficult to differentiate from other ovarian cystic masses (Takeuchi et al., 2015).

Demonstration of hemosiderin deposition reflecting repeated cyclic hemorrhage is also useful for the diagnosis of extra-ovarian endometriosis such as urinary bladder, abdominal wall, etc. as tumor-like masses containing signal voids due to hemosiderin deposition on SWI. Peritoneal implants of endometriosis may appear as small hemosiderin depositions, which are well visualized by the presence of peritoneal fluid collection (Cimsit et al., 2016).

Ectopic pregnancy may appear as complicated heterogeneous mass, which may contain acute, subacute, and chronic hemorrhage exhibiting marked low intensity on SWI. Acute peritoneal hemorrhage may also show low intensity on SWI (*Yoshigi et al.*, 2006).

Adenomyosis with hemorrhagic foci show punctate signal voids due to hemosiderin deposition scattered within adenomyosis. SWI is more sensitive for hemorrhagic foci than fsT1WI, and is useful in differentiating focal adenomyosis from physiologic contraction (Takeuchi et al., 2015).



Red degeneration of uterine leiomyomas is hemorrhagic infarction due to venous obstruction, associated pregnancy, or oral contraceptives is characterized by high intense rim on T1WI corresponding to strongly paramagnetic methemoglobin within obstructed veins which may appear at late phase of red degeneration. At early phase high intense rim on T1WI does not appear yet, however, low intense rim on corresponding deoxyhemoglobin T2WI/SWI to obstructed veins may be observed. This low intense rim due to T2*-shortening effect by deoxyhemoglobin is more prominent on SWI (Byams et al., 2012).

AIM OF THE STUDY

The aim of study is to evaluate the role of susceptibility-weighted images in diagnosis of various gynecologic pathologies by the detection of the presence of internal hemorrhage at any stage.

Chapter 1

ANATOMY OF FEMALE REPRODUCTIVE SYSTEM

The uterus is a pear-shaped muscular organ. It is the site of menstruation, implantation of a fertilized ovum, development of the fetus during pregnancy, and labor. Before the first pregnancy, it measures approximately 3 inches long, 2 inches wide, and 1 inch thick (**Fig. 1**). After a pregnancy, the uterus remains larger than before the pregnancy. After menopause, it becomes smaller and atrophies (*Blackburn et al.*, 2011).

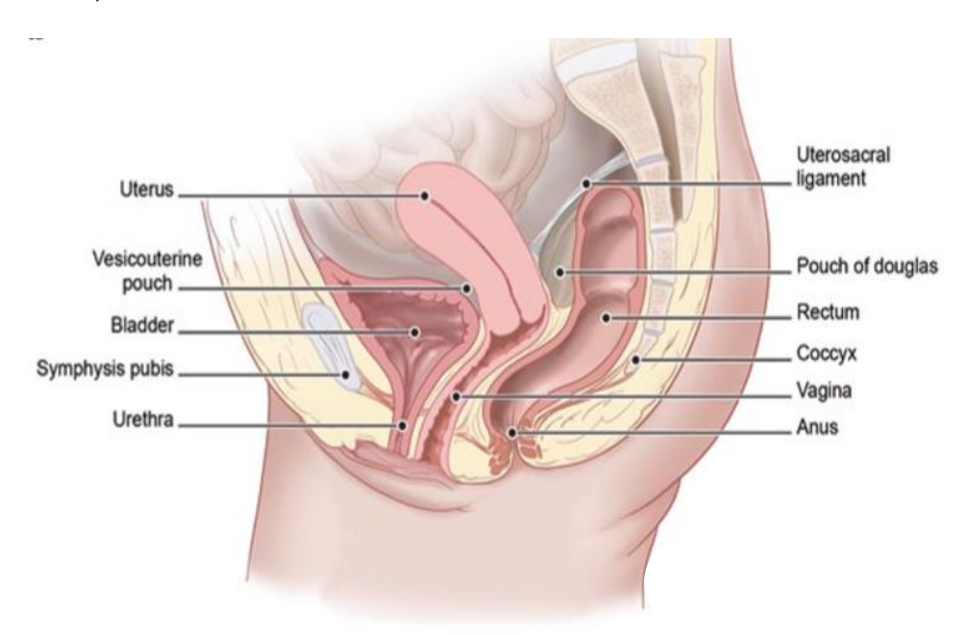


Fig. (1): Female reproductive organs (Blackburn et al., 2011).